




1. Classification <i>INPE-COM.10/PE</i> <i>C.D.U.: 681.3.053</i>	2. Period	4. Distribution Criterion internal <input type="checkbox"/> external <input checked="" type="checkbox"/>
3. Key Words (selected by the author) <i>IMAGE PROCESSING</i> <i>EDGE DETECTION</i> <i>STATISTICAL DECISION THEORY</i>		7. Revised by <i>José Sobral</i> <i>J. H. A. Sobral</i>
5. Report Nº <i>INPE-1206-PE/117</i>	6. Date <i>Março 1978</i>	9. Authorized by  <i>Nelson de Jesus Parada</i> Director
8. Title and Sub-title <i>A BAYESIAN APPROACH TO EDGE DETECTION IN IMAGES</i>		11. Nº of Copies <i>15</i>
10. Sector <i>DSE</i> Code	14. Nº of Pages <i>30</i>	
12. Authorship <i>N.D.A. Mascarenhas</i> <i>L.O.C. Prado</i>  		15. Price
13. Signature of the responsible <i>Nelson de Jesus Parada</i> 16. Summary/Notes <p><i>New statistical techniques for the edge detection problem in images are developed. The image is modeled by signal and noise which are independent, additive, Gaussian and autorregressive in two dimensions. The optimal solution, in terms of statistical decision theory, leads to a test which decides among multiple, composite, overlapping hypotheses. A computationally attractive suboptimal test, involving non-overlapping hypotheses, is proposed. Results are presented with simulated data and real satellite images. A comparison with standard gradient techniques is made.</i></p>		
17. Remarks <i>This work will be submitted for publication in the IEEE Transactions on Automatic Control.</i>		

A BAYESIAN APPROACH TO EDGE DETECTION IN IMAGES

N.D.A. Mascarenhas and L.O.C. Prado⁽¹⁾

Abstract - New statistical techniques for the edge detection problem in images are developed. The image is modeled by signal and noise, which are independent, additive, Gaussian and autorregressive in two dimensions. The optimal solution, in terms of statistical decision theory, leads to a test that decides among multiple, composite, overlapping hypotheses. A redefinition of the problem, involving non-overlapping hypotheses, allows the formulation of a computationally attractive scheme.

Results are presented with both simulated data and real satellite images. A comparison with standard gradient techniques is made.

I. INTRODUCTION

In digital image processing it is often necessary to delineate the boundary between two regions having different gray levels, that remain approximately constant in each region. This computational task of image segmentation is usually called edge detection.

Edge detection may be necessary as a preprocessing operation in automatic pattern recognition systems. Once the boundaries are detected, it is possible to proceed with the classification of the resulting homogeneous regions. Image registration problems are often more

⁽¹⁾ N.D.A. Mascarenhas and L.O.C. Prado are associated with the Instituto de Pesquisas Espaciais (INPE), Conselho Nacional de Desenvolvimento Científico e Tecnológico (CNPq), 12200 - São José dos Campos, SP, Brasil.

N.D.A. Mascarenhas is also associated with the Instituto Tecnológico de Aeronáutica, 12200 - São José dos Campos, SP, Brasil.

Preferred address for correspondence and return of proofs: N.D.A. Mascarenhas, Instituto de Pesquisas Espaciais (INPE), Conselho Nacional de Desenvolvimento Científico e Tecnológico (CNPq), 12200 - São José dos Campos, SP, Brasil. Tel. (0123) 21-8900, ext. 248.

efficiently handled by first detecting the edges in the images. Other applications include data compression for the storage and transmission of images using just their contours. The problem of edge detection is complicated by the inevitable presence of noise. Noise could be due to the electromagnetic sensors and the associated analog electronic circuits that introduce thermal and shot noise; or to the quantization that is necessary for the digital representation of the image; or to graininess of the photographic films, for example.

The present methods for edge detection are often heuristic. The most classical technique is based on the magnitude of the gradient of a function of two spatial variables, which is high in regions corresponding to edges. Operations involving higher order derivatives, such as the Laplacian, have also been considered. A basic problem arising in the application of these techniques using differentiation is their susceptibility to noise in the image. As an attempt to cope with noise, methods that utilize some degree of smoothing like least squares approximations by polynomials could be used. However, this is done at the price of considerable increase of the computation load. For a survey on techniques for edge detection the reader could consult [1]. A few statistical methods for detecting edges have been considered. Nahi and Habibi [2] used a replacement process to decide if a picture element belongs to the object or to the background. Modestino and Fries [3] used two-dimensional recursive digital filtering structures.

The method that is proposed in this article is based on statistical decision theory and it explicitly takes into consideration the randomness of signal and noise. Moreover, the algorithm can be implemented with a computational effort that is at worst comparable to those techniques involving derivatives.

II. STATEMENT OF THE PROBLEM

The statistical algorithm adopts the following two-dimensional autorregressive model for the signal [2]

$$s(k+1, \ell+1) = \rho_1 s(k+1, \ell) + \rho_2 s(k, \ell+1) - \rho_1 \rho_2 s(k, \ell) + \sqrt{(1 - \rho_1^2)(1 - \rho_2^2)} U(k, \ell) \quad (1)$$

In this model, the random variables have null means; $\rho_1(\rho_2)$ is the correlation coefficient between non-noisy pixels in the horizontal (vertical) direction; $\{U(k, \ell)\}$ is a set of non-correlated random variables with the same variance as $\{s(k+1, \ell+1)\}$. The stationarity assumption that is implied by this model may not be strictly true for the whole image, particularly near the edges but, nevertheless, the simplicity of the mathematical model and our experimental results tend to justify this simplifying assumption.

We also adopt the hypothesis that the signal is Gaussian. Although this may not be perfectly accurate, it has often been assumed, particularly for multispectral earth resources imagery [5]. Furthermore, the model has the feature of being easy to determine experimentally, since it only requires estimation of means and covariance between pixels.

The noise of the image might come from several sources, as stated earlier. Some of these sources may be multiplicative and signal dependent but, in order to keep the model tractable, it is convenient to assume that this noise is Gaussian, additive, independent of the signal and also described by Eq. (1). Again, our experimental results tend to confirm that, despite the limitations, the assumption is reasonable.

Once the models for signal and noise are established, the next step is to adequately define the edge-detection problem. This definition should be simple and yet should take into consideration the manner in which humans tend to interpret edges.

With this perspective, the edge detection problem is proposed in the following terms: having observed four noisy pixels $v(i, j)$, $v(i, j+1)$, $v(i+1, j)$ and $v(i+1, j+1)$, as in Fig. (1), where $v(k, \ell) = s(k, \ell) + n(k, \ell)$

(i.e, noisy signal = signal + noise), we want to make a decision about the signal without noise.

This formulation of the problem in terms of statistical decision theory leads to a set of seven possible hypotheses

$$1) \left| s(i,j) - \frac{s(i,j+1)+s(i+1,j)+s(i+1,j+1)}{3} \right| \geq \Delta$$

$$2) \left| s(i,j+1) - \frac{s(i,j)+s(i+1,j)+s(i+1,j+1)}{3} \right| \geq \Delta$$

$$3) \left| s(i+1,j) - \frac{s(i,j)+s(i,j+1)+s(i+1,j+1)}{3} \right| \geq \Delta$$

$$4) \left| s(i+1,j+1) - \frac{s(i,j)+s(i,j+1)+s(i+1,j)}{3} \right| \geq \Delta$$

$$5) \left| \frac{s(i,j)+s(i,j+1)}{2} - \frac{s(i+1,j)+s(i+1,j+1)}{2} \right| \geq \Delta$$

$$6) \left| \frac{s(i,j)+s(i+1,j)}{2} - \frac{s(i,j+1)+s(i+1,j+1)}{2} \right| \geq \Delta$$

$$7) \left| s(i,j) - \frac{s(i,j+1)+s(i+1,j)+s(i+1,j+1)}{3} \right| < \Delta$$

$$\begin{aligned}
 & \bigcap \left| s(i,j+1) - \frac{s(i,j)+s(i+1,j)+s(i+1,j+1)}{3} \right| < \Delta \\
 & \bigcap \left| s(i+1,j) - \frac{s(i,j)+s(i,j+1)+s(i+1,j+1)}{3} \right| < \Delta \\
 & \bigcap \left| s(i+1,j+1) - \frac{s(i,j)+s(i,j+1)+s(i+1,j)}{3} \right| < \Delta \\
 & \bigcap \left| \frac{s(i,j)+s(i,j+1)}{2} - \frac{s(i+1,j)+s(i+1,j+1)}{2} \right| < \Delta \\
 & \bigcap \left| \frac{s(i,j)+s(i+1,j)}{2} - \frac{s(i,j+1)+s(i+1,j+1)}{2} \right| < \Delta \tag{2}
 \end{aligned}$$

The non-negative parameter Δ is chosen by some interaction with the machine through a computer display and allows one to adjust the result of the decision to a visual judgement.

Hypotheses 1 to 6 correspond, respectively, to the existence of edges according to diagonal (Figs. 2 to 5), horizontal (Fig. 6) and vertical (Fig. 7) directions and hypothesis 7 corresponds to the non-existence of an edge.

Proposed as such, the edge detection problem is reduced to the solution of a multiple hypotheses problem. Moreover, these hypotheses are composite (since each of them involves a region in the space of the signal) and they overlap (since, for example, the following set of non-noisy pixels (Fig. 8) satisfies hypotheses 1, 2 and 5, for $\Delta=0.5$).

In the next two sections, several solution methods for this hypothesis testing problem will be developed.

III. OPTIMAL SOLUTION

The statistical decision problem presented in the previous section will be solved by adopting the Bayesian point of view.

Fig. (9) illustrates the diagram of the model. We want to partition the observation space V , that is to choose the optimal decision rule. $\sigma(s)$ defines the probability density function of the non-noisy signal; $f(v/s)$ gives the probability density function of the noisy signal, conditioned upon the value of the non-noisy signal; with respect to the decision rule $d(\gamma/v)$, that assigns a decision $\gamma_i, i=1, \dots, 7$, conditioned upon an observation v , it is well known that nothing is gained by admitting a randomized decision rule. Therefore, the space V will be partitioned in seven regions, corresponding to seven possible decisions.

The overall risk for a decision γ_i is given by

$$R(\gamma_i) = \int_V dv \int_S ds C(s, \gamma_i) f(v/s) \sigma(s) \quad (3)$$

Note that this optimal solution, as is usual in bayesian formulations, depend on the choice of the cost functions $C(\gamma_i, s)$.

This risk will be minimized by selecting the decision γ_i that corresponds to the minimal inner integral given by:

$$A_i(v) = \int_S C(s, \gamma_i) f(v/s) \sigma(s) ds \quad (4)$$

Although the problem is close to the theoretical solution, there is a significant point to be considered: the fact that the hypotheses overlap. One can imagine space S as being partitioned into two regions: a) hypothesis 7 (non-edge), which is disjoint of the other six hypotheses by definition; b) hypotheses 1 to 6, which overlap each other.

Ogg [6] and Middleton [7] proposed the following cost function to solve the overlapping hypotheses testing problem:

$$C(s, \gamma_i) = \frac{\sum_{j=1}^7 c(\gamma_i, j) P_j W_j(s)}{\sum_{j=1}^7 P_j W_j(s)} \quad (5)$$

where $P_j = \int_{\text{region } j} \sigma(s) ds$ is the a priori probability associated with hypothesis j , $W_j(s)$ is the conditional probability density of s , given hypothesis j , and $c(\gamma_i, j)$ is the cost to decide for hypothesis γ_i , when we consider class j .

If we select the following cost functions:

$$c(\gamma_i, j) = \begin{cases} 1 & \text{if } i \neq j \\ 0 & \text{if } i = j \end{cases} \quad (6)$$

it follows that:

$$A_i(v) = \sum_{\substack{j=1 \\ j \neq i}}^7 \int_{\text{region } j} \sigma(s) f(v/s) ds \quad (7)$$

We must take the minimum value for $A_i(v)$, $i = 1, 2, \dots, 7$. It is easy to see that $A_i(v)$ will be minimum if

$\int_{\text{region } i} \sigma(s) f(v/s) ds$ is maximum. The final decision, for the costs

given by (6), would consist in performing seven integrals of the last type and to consider the largest of them.

Although the edge detection problem is now formally solved, there are still computational obstacles that have to be removed. First, integrations in a four-dimensional space must be made. The integration over the region that defines the seventh hypothesis (non-existence of edge) is very difficult to be numerically computed since this region is defined by the intersection of regions, as is clear from Eq. (2).

The next section will show the development of a redefinition of the problem that will circumvent this difficulty.

IV. REDEFINITION OF THE PROBLEM

The computational problems involved in the optimal solution, led us to develop the following scheme: one first makes binary decisions,

involving non-overlapping hypotheses of the type edge versus non-edge of the same type. Then, the results of the preliminary tests are compared and the final decision is made. This scheme is illustrated by Fig.(10).

This type of formulation tends to favor the acceptance of the non-edge hypothesis, for two reasons:

a) the integration $\int_{\text{region non-edge}} \sigma (s) f (v/s) ds$ in each binary decision is

made over a region that is larger than the one that is used in the optimal solution, because in the optimal scheme the region that defines the hypothesis non-edge is an intersection of the non-edge areas. Observe that the regions that define the hypothesis non-edge are different in each of the preliminary tests;

b) the non-edge hypothesis appears in all six preliminary tests, while any other hypothesis shows up in only one of the tests.

This preferential treatment of the non-edge hypothesis can be somehow compensated by making the cost higher for choosing the hypothesis non-edge when the opposite is true in the partial tests.

The derivation of the decision procedure for each binary detection problem can start with Eq. (4) since it does not depend upon whether the hypotheses overlap or not. In this situation, there are two hypotheses, edge of a certain type versus non-edge of the same type and we have two functions $A_1 (v)$ and $A_2 (v)$.

Since the hypotheses do not overlap, one can use as the cost functions $C (s, \gamma_i)$ constant values c_{ij} , where the first and second indexes denote the true and chosen hypothesis, respectively. Index 0 represents hypothesis non-edge of a certain type and index 1 denotes edge of the same type.

Therefore, the final decision is given by:

$$\frac{\int_{|| \geq \Delta} \sigma (s) f (v/s) ds}{\int_{|| < \Delta} \sigma (s) f (v/s) ds} \begin{matrix} 1 \\ > \\ 0 \end{matrix} \frac{C_{01} - C_{00}}{C_{10} - C_{11}} \quad (8)$$

where 1 denotes decision for an edge of a certain type and 0 denotes decision for no edge.

Therefore, the classical Bayesian test that decides between two composite hypotheses, involving a likelihood ratio, is obtained [8].

Once the binary decisions, involving edge versus non-edge of a certain type, are made, the final decision about which type of edge (or non-edge) is chosen (Fig. 10) has to be made. For this, we will associate with the accepted hypothesis in the preliminary test the value

$$\frac{C_{10} - C_{11}}{C_{01} - C_{00}} \begin{cases} \int \sigma(s) f(v/s) ds \\ || \geq \Delta \\ \hline \int (s) f(v/s) ds \\ || < \Delta \end{cases} \quad (9)$$

or its reciprocal, depending on whether this value is not less (there is an edge) or less (there is no edge) than one.

We will accept the hypothesis that is associated with the highest value. Observe that the hypothesis non-edge can furnish up to six candidates for the final decision.

In section II, the signal and noise were both modeled as Gaussian processes. It is possible to specify the test given by Eq. (8) in this particular case. We must then give the vector of expected values and the covariance matrix.

The model for the non-noisy signal, given by Eq. (1), admits zero mean. In order for this model to reflect reality it is necessary to subtract the sample mean from the image before the processing is made.

From the separability of the correlation structure of the process on the horizontal and vertical directions, it follows that the covariance matrix is given by the Kronecker product of two matrices [9] so that

$$\begin{aligned} \underline{C}_S &= \sigma^2 \left(\begin{pmatrix} 1 & \rho_1 \\ \rho_1 & 1 \end{pmatrix} \otimes \begin{pmatrix} 1 & \rho_2 \\ \rho_2 & 1 \end{pmatrix} \right) \\ &= \sigma^2 \begin{pmatrix} 1 & \rho_2 & \rho_1 & \rho_1\rho_2 \\ \rho_2 & 1 & \rho_1\rho_2 & \rho_1 \\ \rho_1 & \rho_1\rho_2 & 1 & \rho_2 \\ \rho_1\rho_2 & \rho_1 & \rho_2 & 1 \end{pmatrix} \end{aligned} \quad (10)$$

where σ^2 is the variance of the non-noisy signal and $\rho_1(\rho_2)$ is the correlation coefficient between adjacent pixels on the horizontal (vertical) direction.

The same structure is assumed for the covariance matrix of the noise, which is also supposed to have zero mean. It follows that

$$\underline{C}_N = \sigma_N^2 \left(\begin{pmatrix} 1 & \rho_{1N} \\ \rho_{1N} & 1 \end{pmatrix} \otimes \begin{pmatrix} 1 & \rho_{2N} \\ \rho_{2N} & 1 \end{pmatrix} \right) \quad (11)$$

One can then write the expression for $\sigma(s)$ as

$$\begin{aligned} \sigma(s) &= \frac{1}{(2\pi)^2 |\underline{C}_S|^{1/2}} \exp \left[-\frac{1}{2} (s(i,j) \ s(i,j+1) \ s(i+1,j) \ s(i+1,j+1)) \right. \\ &\quad \left. \underline{C}_S^{-1} (s(i,j) \ s(i,j+1) \ s(i+1,j) \ s(i+1,j+1))^T \right] \end{aligned} \quad (12)$$

and for f (v/s) as

$$f(v/s) = \frac{1}{(2\pi)^2 |\underline{C}_N|^{1/2}} \exp \left[-\frac{1}{2} \begin{pmatrix} v(i,j)-s(i,j) & v(i,j+1)-s(i,j+1) \\ v(i+1,j)-s(i+1,j) & v(i+1,j+1)-s(i+1,j+1) \end{pmatrix} \underline{C}_N^{-1} \begin{pmatrix} v(i,j)-s(i,j) & v(i,j+1)-s(i,j+1) \\ v(i+1,j)-s(i+1,j) & v(i+1,j+1)-s(i+1,j+1) \end{pmatrix}^T \right] \quad (13)$$

In order to determine \underline{C}_S^{-1} and \underline{C}_N^{-1} it is only necessary to compute inverses of matrices of dimension two, due to the result [10]:

$$(A \otimes B)^{-1} = A^{-1} \otimes B^{-1} \quad (14)$$

The computational implementation of the likelihood ratio test may demand the construction and the use of tables, which avoids the necessity of repeating the numerical calculation of the integrals.

From the symmetry of the problem, it is only necessary to compute the two tables corresponding to hypothesis 1 and 5 (edges at 45° and horizontal). However, these tests depend on tables with four entry variables and this computational effort may make the algorithm unfeasible in practice. In the next section the development of a computationally attractive approximation to the redefinition of the problem is introduced.

V. APPROXIMATION ON THE REDEFINITION OF THE PROBLEM

In order to make feasible the solution to the edge detection problem, it is necessary to make a new approximation. Rather than examine the four noisy pixels in order to make the decision, only two random variables will be observed.

Therefore, to decide edge of type 1 against non-edge of type 1 (edge at 45°), instead of observing $v(i,j)$, $v(i, j+1)$, $v(i+1, j)$ and $v(i+1, j+1)$, only $v(i, j)$ and $\frac{v(i, j+1) + v(i+1, j) + v(i+1, j+1)}{3}$ will be observed. Likewise, in

the test of edge of type 5 (horizontal edge) versus non-edge of the same type, the likelihood functions will depend on $\frac{v(i, j) + v(i, j+1)}{2}$ and $\frac{v(i+1, j) + v(i+1, j+1)}{2}$. As a result, the necessary tables will depend on only two variables, which considerably reduces the computational task.

Therefore, in the case of edge of type 1, the denominator of expression (8) assumes the form:

$$\int_{|| < \Delta} \sigma(s(i, j), s(i, j+1), s(i+1, j), s(i+1, j+1)) f\left(\frac{v(i, j) + v(i, j+1) + v(i+1, j) + v(i+1, j+1)}{3} \mid s(i, j), s(i, j+1), s(i+1, j), s(i+1, j+1)\right) ds(i, j) ds(i, j+1) ds(i+1, j) ds(i+1, j+1) \quad (15)$$

Specializing the previous equation in the Gaussian case, it follows that

$$\int_{|| < \Delta} \frac{1}{(2\pi)^2 |\underline{C}_S|^{1/2}} \exp\left[-\frac{1}{2} (s(i, j) \ s(i, j+1) \ s(i+1, j) \ s(i+1, j+1)) \underline{C}_S^{-1} (s(i, j) \ s(i, j+1) \ s(i+1, j) \ s(i+1, j+1))^T\right] \frac{1}{2\pi |\underline{C}_{NT}|^{1/2}} \exp\left[-\frac{1}{2} (v(i, j) - s(i, j) - \frac{v(i, j+1) + v(i+1, j) + v(i+1, j+1)}{3} - \frac{s(i, j+1) + s(i+1, j) + s(i+1, j+1)}{3}) \underline{C}_{NT}^{-1} (v(i, j) - s(i, j) - \frac{v(i, j+1) + v(i+1, j) + v(i+1, j+1)}{3} - \frac{s(i, j+1) + s(i+1, j) + s(i+1, j+1)}{3})^T\right] ds(i, j) ds(i, j+1) ds(i+1, j) ds(i+1, j+1) \quad (16)$$

where [11]

$$C_{NT} = T C_N T^T \quad (17)$$

and

$$T = \begin{pmatrix} 1 & 0 & 0 & 0 \\ 0 & 1/3 & 1/3 & 1/3 \end{pmatrix}$$

VI. SIMPLIFICATION OF THE INTEGRALS COMPUTATION

Let us assume the following notation:

$$s_1 = s(i, j)$$

$$s_2 = s(i, j+1)$$

$$s_3 = s(i+1, j)$$

$$s_4 = s(i+1, j+1)$$

$$s' = \frac{s_2 + s_3 + s_4}{3}$$

$$v_1 = v(i, j)$$

$$v' = \frac{v(i, j+1) + v(i+1, j) + v(i+1, j+1)}{3}$$

Under these conditions, expression (15) assumes the form:

$$\int \int \int \int f(v_1, v' | s_1 s_2 s_3 s_4) f_{S_1 S_2 S_3 S_4}(s_1, s_2, s_3, s_4) \cdot \left| s_1 - \frac{s_2 + s_3 + s_4}{3} \right| < \Delta \quad (18)$$

$$ds_1 ds_2 ds_3 ds_4$$

In Appendix A we show that, in the Gaussian case, expression (18) can be obtained by performing only a double integration, instead of

quadruple integration, that is, Eq. (18) can be given by:

$$\int_{-\infty}^{\infty} ds_1 \int_{s_1-\Delta}^{s_1+\Delta} ds' f(v_1, v' | s_1, s') f_{S_1 S'}(s_1, s') \quad (19)$$

This result considerably reduces the computational effort of numerical integration. Therefore, by explicitly denoting the Gaussian densities, Eq. (19) is given by:

$$\int_{-\infty}^{+\infty} ds_1 \int_{s_1-\Delta}^{s_1+\Delta} ds' \frac{1}{2\pi |C_{NT}|^{1/2}} \exp \left[-\frac{1}{2} (v_1-s_1 \ v'-s') \underline{C}_{NT}^{-1} (v_1-s_1 \ v'-s')^T \right]$$

$$\frac{1}{2\pi |C_{ST}|^{1/2}} \exp \left[-\frac{1}{2} (s_1 \ s') \underline{C}_{ST}^{-1} (s_1 \ s')^T \right] \quad (20)$$

where

$$\underline{C}_{ST} = \underline{I} \underline{C}_S \underline{I}^T \quad (21)$$

Observe that the simplification performed in this section does not introduce any new approximation on the solution in the Gaussian case.

VII. NUMERICAL COMPUTATION OF THE INTEGRALS

Eq. (8) specifies the likelihood ratio test, which requires the computation of integrals in the numerator and the denominator.

The denominator, given by

$$\int_{|| < \Delta} \sigma(s) f(v/s) ds, \text{ can be calculated by}$$

$$\int_{-\infty}^{\infty} ds_{\alpha} \int_{s_{\alpha}-\Delta}^{s_{\alpha}+\Delta} ds_{\beta} \sigma(s_{\alpha}, s_{\beta}) f(v_{\alpha}, v_{\beta} | s_{\alpha}, s_{\beta}) \quad (22)$$

where

$$v_{\alpha} = v(i, j)$$

$$s_{\alpha} = s(i, j)$$

$$v_{\beta} = \frac{v(i, j+1) + v(i+1, j) + v(i+1, j+1)}{3}$$

$$s_{\beta} = \frac{s(i, j+1) + s(i+1, j) + s(i+1, j+1)}{3}$$

in the case of the test for an edge of type 1 (diagonal edge), for example. An analogous expression is used with tests type 2, 3 and 4.

For test type 5 (horizontal edge), we have

$$v_{\alpha} = \frac{v(i, j) + v(i, j+1)}{2}$$

$$s_{\alpha} = \frac{s(i, j) + s(i, j+1)}{2}$$

$$v_{\beta} = \frac{v(i+1, j) + v(i+1, j+1)}{2}$$

$$s_{\beta} = \frac{s(i+1, j) + s(i+1, j+1)}{2}$$

An analogous convention can be used with test type 6 (vertical edge). The numerator of Eq. (8), given by

$$\int_{|| \geq \Delta} \sigma(s) f(v/s) ds, \text{ can be calculated by}$$

$$\int_{-\infty}^{+\infty} ds_{\alpha} \int_{-\infty}^{s_{\alpha} - \Delta} ds_{\beta} \sigma(s_{\alpha}, s_{\beta}) f(v_{\alpha}, v_{\beta} | s_{\alpha}, s_{\beta}) +$$

$$\int_{-\infty}^{+\infty} ds_{\alpha} \int_{s_{\alpha} + \Delta}^{+\infty} ds_{\beta} \sigma(s_{\alpha}, s_{\beta}) f(v_{\alpha}, v_{\beta} | s_{\alpha}, s_{\beta}) \quad (23)$$

In the following we shall present the general scheme of numerical integrations of expressions (22) e (23).

Under the hypothesis of signal and noise being Gaussian, those integrals have the general form.

$$K \cdot \int_{-\infty}^{+\infty} dx \exp(-x^2) \frac{1}{\sqrt{2\pi}} \int_a^b \exp(-y^2/2) dy \quad (24)$$

In the case of Eq. (22), a and b are finite; in the first term of Eq. (23), a = -∞ and b is finite, while in the second term, a is finite and b = +∞.

The integration

$$\frac{1}{\sqrt{2\pi}} \int dy \exp(-y^2/2) \quad \text{is performed by storing a Gaussian distribution}$$

table. The integration from -∞ to +∞ then can be put in the form:

$$K \cdot \int_{-\infty}^{+\infty} dx \exp(-x^2) f(x) \quad (25)$$

This integral can be numerically calculated through the application of the Gauss-Hermite formula [12]:

$$\int_{-\infty}^{+\infty} dx \exp(-x^2) f(x) \cong \sum_{K=1}^m H_K f(x_K) \quad (26)$$

where x_K is the K-th zero of the Hermite polynomial $H_m(x)$ of the m^{th} degree and the weights H_K are given by:

$$H_K = \frac{2^m (m-1)! \sqrt{\pi}}{H'_m(x_K) H_{m-1}(x_K)} \quad (27)$$

Values of x_K and H_K are given by tables [13].

VIII. EXPERIMENTAL RESULTS

To test the proposed algorithm simulation work was performed on a cartoon image of size 128x128 pixels with 9 gray levels (Fig. 11). White gaussian noise was added to the image, under different signal to noise ratios; 20 roots were used when performing the Gauss-Hermite integration and a normal distribution with precision up to 6.8 standard deviations was stored.

The number of hypotheses were reduced from 7 to 5, in order to avoid an excessive amount of computation, according to Figs. 12, 13, 14 and 15. Hypothesis 5 corresponds to non-existence of edge. There was overlapping of two pixels in two groups of four pixels that were examined on the horizontal and vertical directions. The scheme for darkening the pixels in this simulation work is indicated by the circles in the previously mentioned figures. Despite the overlapping in the groups of pixels, no change in the darkening of pixels was made after the decision was taken.

The results with SNR (that is, the ratio of signal variance to noise variance) 100 (Figs. 16 and 17), 30 (Figs. 18 and 19), 10 (Figs. 20 and 21) and using the correlation coefficient of the signal equal to 0,96 (estimated from the original image), show that the algorithm is able to cope with noise quite effectively.

Decreasing the SNR further (SNR = 5) (Figs. 22 and 23), there is a tendency for the edges to disappear. This can be interpreted in terms of the fact that, for those values of the parameters, $P(D_0|H_1)$ is much higher than $P(D_1|H_0)$ in the binary tests, besides the preference given to the non-edge hypothesis, by being present in all these partial tests. This problem was solved by increasing the value of the cost C_{10} from 1.0 to 1.5 (see Fig. 24).

A comparison of the results of the proposed algorithm with the gradient procedure under SNR = 5 is made in Figs. 25 and 26. In Fig. 25 the threshold of the gradient was low (90) and although more edges are picked than the proposed method, there is considerable sensitivity to noise. The best result with the gradient (Fig. 26) was obtained with a threshold of 200 and it can be observed that some loss of edges occurs on the top of the house, the head of the figure and on the boundary of the tree and the cloud, as compared to Fig. 24.

The CPU time for the 128 x 128 pixels image, using the overlapping scanning method with 5 hypotheses, in a B-6700 machine and Algol language, was 380 seconds when performing the likelihood ratios repeatedly by calculation, but this time was reduced to 24 seconds by the use of look-up tables.

The corresponding gradient procedure took 19 seconds. However, in the proposed method, the edges are indicated by a gray level that depends on the ratio of the two greatest likelihood ratios of the partial tests. If we simply associate a dark tone to the existence of an edge and a light tone to the non-existence, it is possible to store in the look-up table only the information of which edge is decided and that requires only one entry (instead of four) in a table that uses a maximum of 3 bits of storage per pair of values, with substantial reduction of computational effort.

The proposed algorithm, under 5 hypotheses with overlap, was applied to detect edges on a 512 x 512 pixels NOAA-V meteorological satellite picture (Fig. 27) with 32 (Fig. 28) and 8 (Fig. 29) levels of quantization, using as parameters $\rho_S = 0,90$, $\rho_N = 0$, $SNR = 60$ (the difference due to a greater quantization noise with 8 levels was not considered), $C_{10} = 10$, $\Delta = 0,90$ (32 levels) and $\Delta = 0,35$ (8 levels). These results show that, by attempting to preserve the number of quantization levels, some continuity of the edges seem to be lost. The correlation coefficient (assumed equal on the horizontal and vertical direction) as well as the signal variance were estimated on an average basis over the whole image with 32 levels. The noise level was determined experimentally by estimating the variance of areas of approximately equal reflectance, like the surface of the ocean, in similar pictures. No artificial noise was added on the processing of the satellite images.

The construction of the table took approximately 2 minutes for 32 levels, while the execution time on a PDP 11/45 in FORTRAN took 20 minutes. The limited precision of the Gaussian table and of the floating point representation of the minicomputer forced some approximations.

IX. CONCLUDING REMARKS

A new algorithm to detect edges in images was developed, under the framework of statistical decision theory. The scheme takes into consideration the randomness of signal and noise. A redefinition of the problem was proposed, with computational effort at least comparable to the classical procedures like the gradient, and better performance under noisy conditions.

It is possible to extend this work in several directions: a) by taking context into consideration, and conditioning the decision upon what is decided on a neighbourhood; b) by considering the blurring in satellite pictures due to atmospheric turbulence or limited sensor resolution, for example; c) by considering a definition of an edge that would include the multispectral character of earth resources or meteorological imagery.

ACKNOWLEDGEMENTS

The authors wish to thank Dr. José M.A. Sobral for his useful comments about the paper and Mr. José Carlos Moreira for his help in the programming of the algorithm.

REFERENCES

- [1] A. Rosenfeld and A.C. Kak, "*Digital Picture Processing*," Academic Press, New York, 1976, ch. 8.
- [2] N.E. Nahi and A. Habibi, "Decision-Directed Recursive Image Enhancement", *IEEE Transactions on Circuits and Systems*, Vol. CAS-22, No 3, March 1975, pp. 286-293.
- [3] J.W. Modestino and R.W. Fries, "Edge Detection in Noisy Images Using Recursive Digital Filtering", *Computer Graphics and Image Processing*, Vol. 6, No 5, 1977, pp. 409-433.
- [4] A. Habibi, "Two Dimensional Bayesian Estimate of Images", *Proceedings of the IEEE*, Vol. 60, No 7, 1972, pp. 878-883.
- [5] R.B. Crane, W.A. Malila and W. Richardson, "Suitability of the Normal Density Assumption Likelihood for Processing Multispectral Scanner Data", *IEEE Transactions on Geoscience Electronics*, Vol. GE-10, No 4, 1972, pp. 158-165.
- [6] F.C. Ogg, Jr., "A Note on Bayes Detection of Signals", *IEEE Transactions on Information Theory*, Vol. 10, No 1, 1964, pp. 57-60.
- [7] D. Middleton, "*Topics in Communication Theory*", Mc Graw Hill, New York, 1965, pp. 22-23.
- [8] A.D. Whalen, "*Detection of Signals in Noise*", Academic Press, 1971, pp. 125-154.
- [9] J.A. Stuller and B. Kurz, "Two Dimensional Markov Representations of Sampled Images", *IEEE Transactions on Communication Theory*, Vol. 24, No 10, October 1976, pp. 1148-1152.
- [10] F.A. Graybill, "*Introduction to Matrices with Applications to Statistics*", Wadsworth, Belmont, California, 1969, pg. 204.
- [11] W.B. Davenport, "*Probability and Random Process: An Introduction for Applied Scientists and Engineers*", Mc Graw Hill, New York, 1970, pg. 348.
- [12] F.B. Hildebrand, "*Introduction to Numerical Analysis*", Mc Graw Hill, New York, 1956, pp. 324-330.
- [13] M. Abramowitz and I. Stegun, "*Handbook of Mathematical Functions*", Dover, New York, 1965.

APPENDIX

We shall show that in the Gaussian case, expression (18) can be given by a double integration.

First, observe that, in the Gaussian case:

$$f(v_1, v' \mid s_1, s_2, s_3, s_4) = f(v_1, v' \mid s_1, s') \quad (A1)$$

since s_1, s_2, s_3 and s_4 only appear in this Gaussian conditional probability density in the form of s_1 and

$$\frac{s_2 + s_3 + s_4}{3} = s', \text{ and since}$$

$$f(v_1, v' \mid s_1, s_2, s_3, s_4) = K \cdot \exp\left[-\frac{1}{2} (v_1 - s_1 \ v' - s')\right. \\ \left. C_{NT}^{-1} (v_1 - s_1 \ v' - s')^T\right] \quad (A2)$$

it is enough then to show that

$$\int \int \int \int f_{s_1 s_2 s_3 s_4}(s_1, s_2, s_3, s_4) ds_1 ds_2 ds_3 ds_4 \cdot \\ \frac{|s_1 - (s_2 + s_3 + s_4)|}{3} < \Delta \\ = \int_{-\infty}^{+\infty} ds_1 \int_{s_1 - \Delta}^{s_1 + \Delta} f_{s_1 s_2}(s_1, s') \quad (A3)$$

For this, let us calculate initially the distribution function $F_{S_1 S'}(s_1, s')$:

$$F_{S_1 S'}(s_1, s') = P[S_1 \leq s_1, S' \leq s'] = \\ = \int_{-\infty}^{s_1} ds_1' \int_{-\infty}^{+\infty} ds_4 \int_{-\infty}^{+\infty} ds_3 \int_{-\infty}^{3s' - s_3 - s_4} ds_2 f_{s_1 s_2 s_3 s_4}(s_1', s_2, s_3, s_4) \quad (A4)$$

Now determining $f_{S_1 S'}(s_1, s')$:

$$\begin{aligned}
 f_{S_1 S'}(s_1, s') &= \frac{\partial^2 F_{S_1 S'}(s_1, s')}{\partial s_1 \partial s'} = \\
 &= \frac{\partial}{\partial s_1} 3 \int_{-\infty}^{s_1} \int_{-\infty}^{+\infty} \int_{-\infty}^{+\infty} f_{S_1 S_2 S_3 S_4}(s_1', 3s' - s_3 - s_4, s_3, s_4) ds_1' ds_3 ds_4 \\
 &= 3 \int_{-\infty}^{+\infty} \int_{-\infty}^{-\infty} f_{S_1 S_2 S_3 S_4}(s_1, 3s' - s_3 - s_4, s_3, s_4) ds_3 ds_4 \quad (A5)
 \end{aligned}$$

Thus, substituting (A5) into (19), we obtain:

$$\begin{aligned}
 &\int_{-\infty}^{+\infty} ds_1 \int_{s_1 - \Delta}^{s_1 + \Delta} ds' f_{S_1 S'}(s_1, s') = \\
 &= \int_{-\infty}^{+\infty} ds_1 \int_{s_1 - \Delta}^{s_1 + \Delta} ds' 3 \int_{-\infty}^{+\infty} \int_{-\infty}^{+\infty} f_{S_1 S_2 S_3 S_4}(s_1, 3s' - s_3 - s_4, s_3, s_4) ds_3 ds_4 \quad (A6)
 \end{aligned}$$

But:

$$3s' - s_3 - s_4 = s_2 \quad (A7)$$

$$3ds' = ds_2$$

so thus, it follows that:

$$\begin{aligned}
 &\int_{-\infty}^{+\infty} ds_1 \int_{-\infty}^{+\infty} ds_3 \int_{-\infty}^{+\infty} ds_4 \int_{3s_1 - s_3 - s_4 - 3\Delta}^{3s_1 - s_3 - s_4 + 3\Delta} ds_2 f_{S_1 S_2 S_3 S_4}(s_1, s_2, s_3, s_4) = \\
 &= \int \int \int \int f_{S_1 S_2 S_3 S_4}(s_1, s_2, s_3, s_4) ds_1 ds_2 ds_3 ds_4 \quad (A8)
 \end{aligned}$$

$$\left| s_1 - \frac{s_2 + s_3 + s_4}{3} \right| < \Delta$$

q.e.d.



Fig. 1 - Set of Pixels for Edge Detection

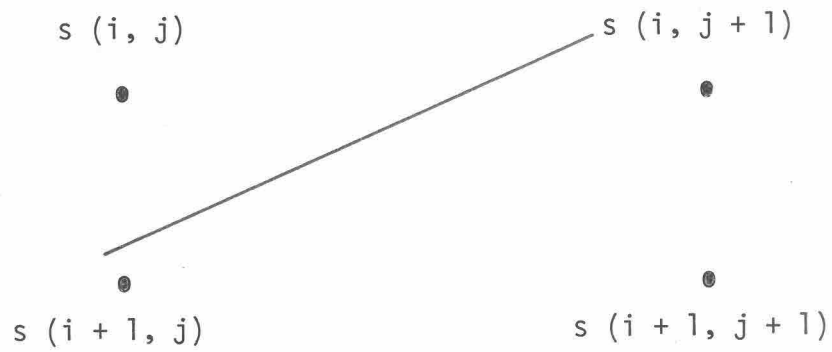


Fig. 2 - Edge of the 1st Type (diagonal)

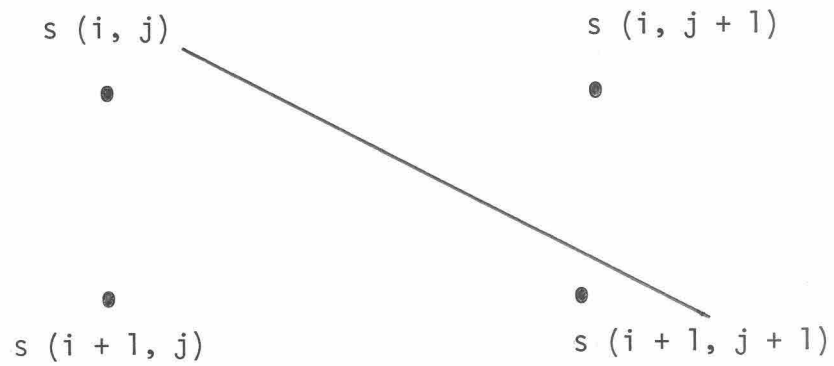


Fig. 3 - Edge of the 2nd Type (diagonal)

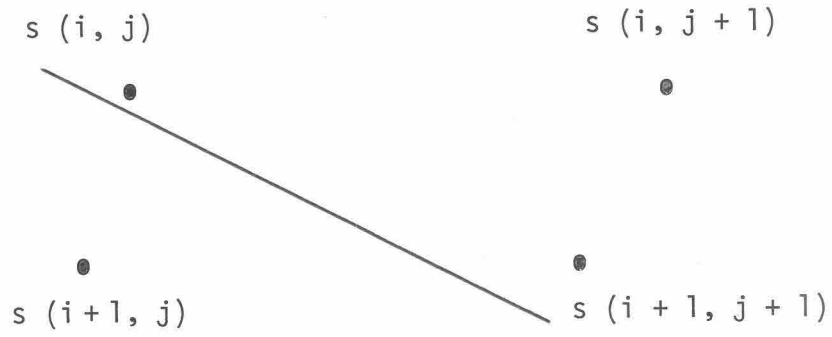


Fig. 4 - Edge of the 3rd Type (diagonal)

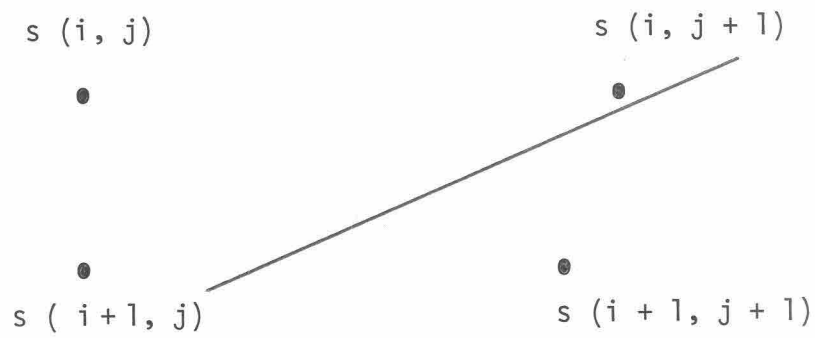


Fig. 5 - Edge of the 4th Type (diagonal)

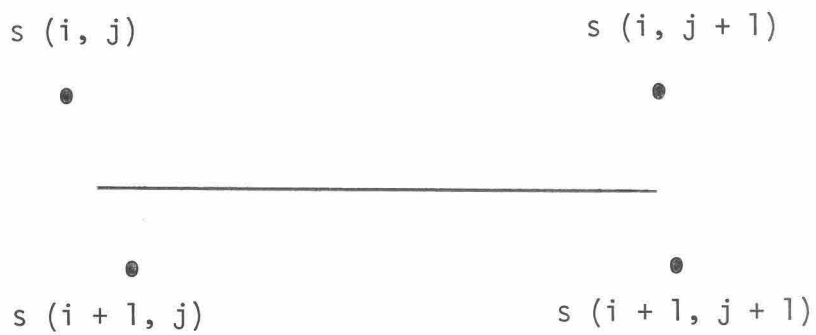


Fig. 6 - Edge of the 5th Type (horizontal)



Fig. 7 - Edge of the 6th Type (vertical)



Fig. 8 - Example of Overlapping of Hypotheses

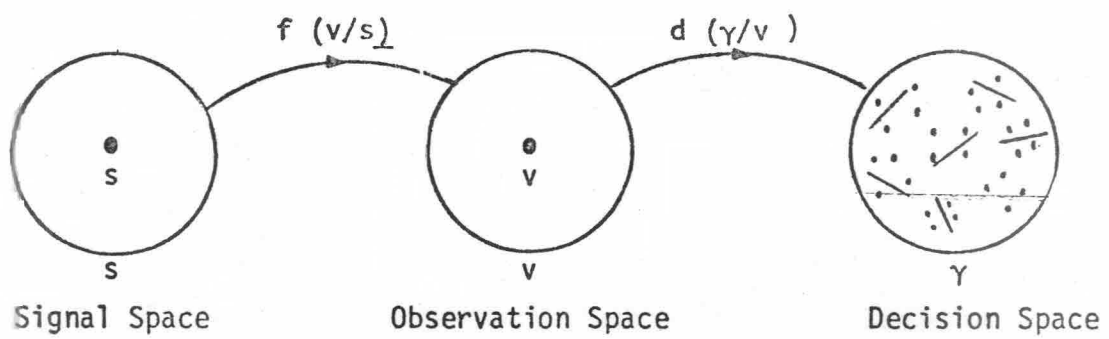


Fig. 9 - Spaces for the Detection Problem

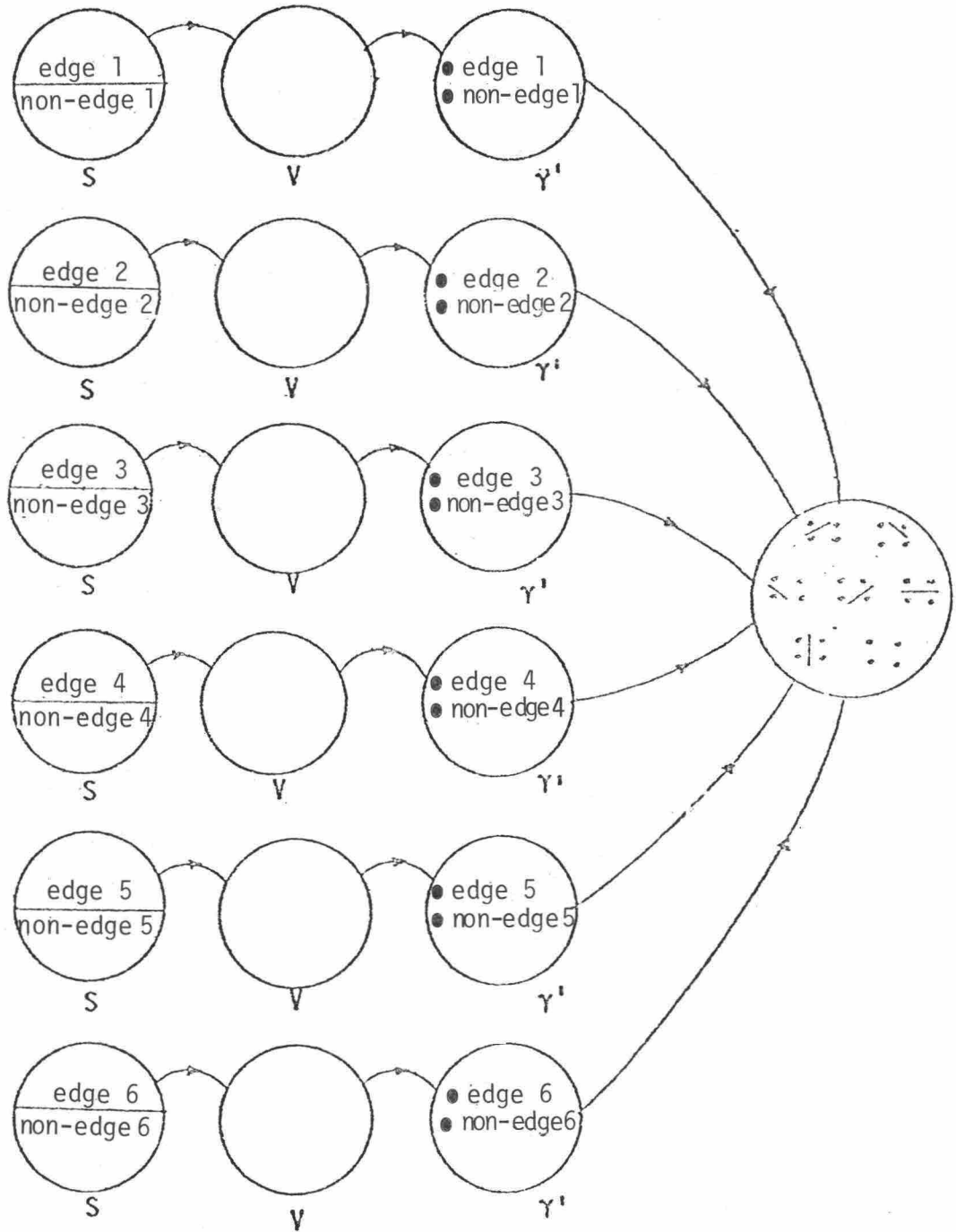


Fig. 10 - Diagram of the Model for Suboptimal Scheme

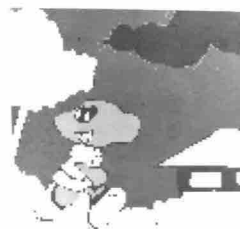


Fig. 11
Original
Cartoon
Image

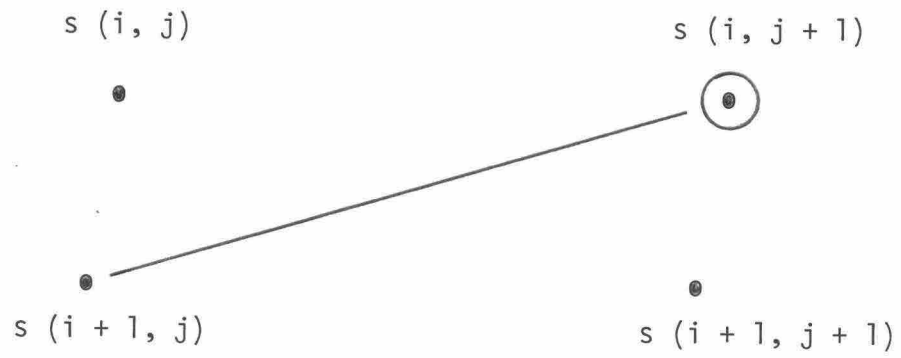


Fig. 12 - Edge of the 1st Type (diagonal)

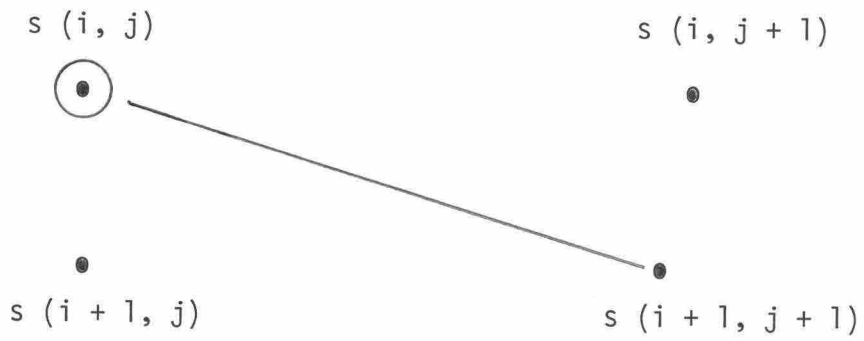


Fig. 13 - Edge of the 2nd Type (diagonal)

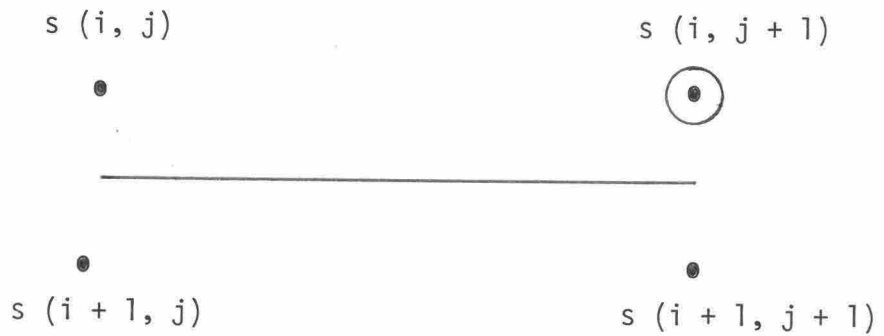


Fig. 14 - Edge of the 3rd Type (horizontal)

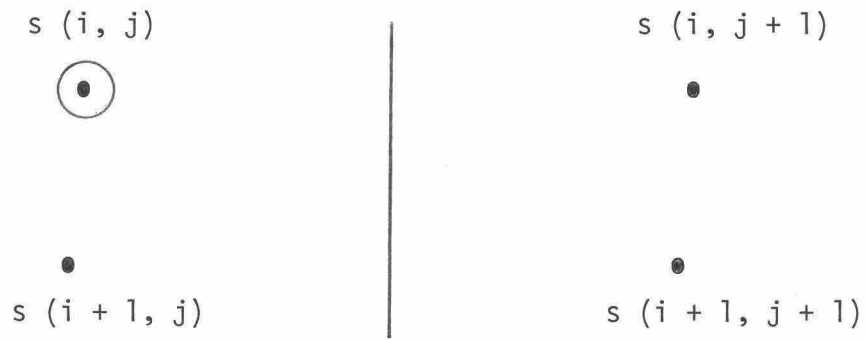


Fig. 15 - Edge of the 4th Type (vertical)

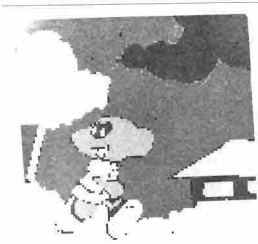


Fig. 16
Cartoon
Image
SNR = 100

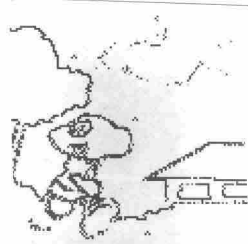


Fig. 17
Edges in
Cartoon
Image
SNR = 100



Fig. 18
Cartoon
Image
SNR = 30



Fig. 19
Edges in
Cartoon
Image
SNR = 30



Fig. 20
Cartoon
Image
SNR = 10



Fig. 21
Edges in
Cartoon
Image
SNR = 10



Fig. 22
Cartoon
Image
SNR = 5

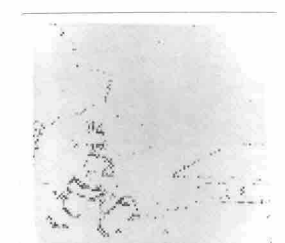


Fig. 23
Edges in
Cartoon
Image
SNR = 5
 $C_{10} = 1$

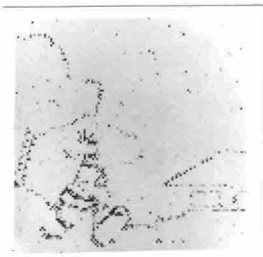


Fig. 24
Edges in
Cartoon
Image
SNR = 5
 $C_{10} = 1.5$

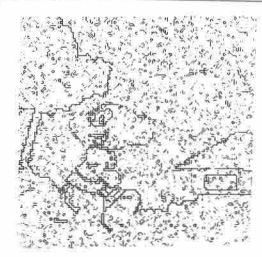


Fig. 25
Gradient
SNR = 5
Threshold = 90

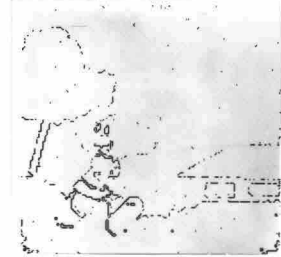


Fig. 26
Gradient
SNR = 5
Threshold = 200

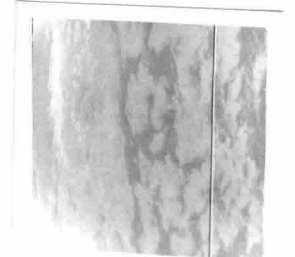


Fig. 27
Satellite
Picture



Fig. 28
Edges in
Satellite
Picture
(32 Levels)

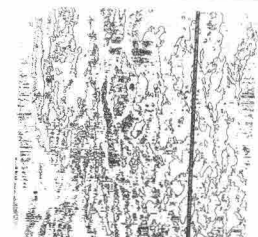


Fig. 29
Edges in
Satellite
Picture
(8 Levels)